

Three Dimensional Finite Element Analysis and Back-analysis of CFA Standard Pile Groups and Piled Rafts Founded on Tropical Soil

Tomás Janda, Renato Pinto da Cunha, Pavel Kuklík, Gérson Miranda dos Anjos

Abstract. This paper deals with Plaxis 3D finite element simulations of the mechanical response of deep foundations founded in a collapsible tropical soil. Main attention is initially paid to differences between single continuous flight auger (CFA) pile behavior and the behavior of CFA piles in standard groups. The numerically computed load-settlement curves are compared to field load test data obtained at the experimental research site of the University of Brasília (UnB), leading to conclusions about the appropriateness of adopting laboratory, *in situ* or back calculated parameters as input of numerical programs that simulate 3D foundation systems. Further, the contribution of the contact surficial soil/top raft is numerically examined by simulating the behavior of identical “piled raft” systems founded in the same site. The numerical simulated results of “piled raft” and standard pile group systems are then compared in terms of load capacity, system stiffness, load share between pile tip, shaft and raft, and mean developed lateral pile shaft friction. Having the results at distinct loading stages, as at working and failure levels, the analyses show the differential behavior, and design obtained responses, one may expect from conventional pile groups and “piled rafts” of CFA floating piles when founded in tropical soils. It is a mixed theoretical/experimental paper with practical interest for foundation designers and constructors.

Key words: pile group, piled raft, numerical analysis, finite element method, settlement, collapsible soil, load distribution, Mohr-Coulomb model.

1. Introduction

Local practice in the Federal District of Brazil shows that one of the most economical types of foundations that can be used to sustain loads from elements founded on tropical unsaturated, or saturated, soils is the continuous flight auger (CFA) pile. Hence, CFA piles are frequently used in foundation systems within the city of Brasília as well as adjacent areas (even in other cities as Goiânia, for instance). Due to their relatively small diameter when compared to traditional large scale bored piles the CFA foundations are, almost in all cases, constructed in groups with a relatively small spacing pile to pile (2 to 3 diameters, in general). The understanding of the entire foundation system requires knowledge not only about the single pile interaction with the soil environment, but also the mutual influence of individual piles within the group. The complexity of the problem does not end here, especially when the pile group supports a top raft, or capped block, which is in close contact with the surficial soil. Since both structural parts of the foundation - piles and raft - need to be considered for a proper understanding of the problem, major attention must be given to numerical techniques which are capable of properly simulating the behavior of the whole foundation system, taking on account the real geometry and individual characteristics, plus the complex interactions between structural and geotechnical elements of the founda-

tion. It is, basically, a question related to the understanding of the behavior of a “piled raft” system, rather than a traditional pile group.

In the past decade several papers have been published with emphasis on what are now called “piled-rafts”, *i.e.*, pile groups in which the raft connecting the pile heads positively contributes to the overall foundation behavior (for example Ottaviani, 1975; Randolph, 1994, Mandolini & Viggiani, 1997, Poulos, 1998; Cunha & Sales, 1998 and Sales *et al.*, 1999). Other more recent papers have expanded upon these initial ideas, such as those by Cunha *et al.* (2000a and b, 2001, 2004, 2006), Sales *et al.* (2005), and Cunha & Zhang (2006). One should however realize that the term “piled raft” is expressed in the present and at all aforementioned papers as a “foundation system in which both structural components (piles and top raft) interact with each other and with the surrounding soil to sustain vertical, horizontal or moment loads coming from supported superstructures”. Independently if the piles are designed as “settlement reducers” or not, piled rafts will be defined herein (and in future papers) by the basic statement previously cited. In fact, according to Mandolini (2003), piled rafts can be designed under a “capacity and settlement based design”, “capacity based design” or as “differential settlement based design”. It is then important to mention that aforementioned definition is unquestionable valid to describe piled

Tomás Janda, MSc., Department of Mechanics CTU, Faculty of Civil Engineering, Thákurova 7, 166 29 Praha 6, Prague, Czech Republic. e-mail: tomas.janda@fsv.cvut.cz.
Renato Pinto da Cunha, Ph.D., Departamento de Engenharia Civil e Ambiental, Universidade de Brasília, Asa Norte, Brasília, DF, Brazil. e-mail: rpcunha@unb.br.
Pavel Kuklík, Doctor, Department of Mechanics CTU, Faculty of Civil Engineering, Thákurova 7, 166 29 Praha 6, Prague, Czech Republic. e-mail: kuklikpa@fsv.cvut.cz.
Gérson Miranda dos Anjos, D.Sc., Faculdade de Engenharia Civil, Universidade Federal do Pará, Belém, PA, Brazil. e-mail: anjosmiranda@hotmail.com.
Submitted on November 29, 2007; Final Acceptance on July 3, 2008; Discussion open until August 31, 2009.

rafts designed in any of the possible criteria established by this latter author.

On the other hand, standard or traditional pile groups are those in which, by design considerations or simply by physical aspects (as the experimental tests of this paper), no superstructure load is supported by the soil underneath the raft, or by the raft itself. In other words, the entire vertical or horizontal load is solely supported by the structural pile elements and their surrounding soil at shaft and base. In this case the raft merely serves as a structural element to distribute the load between pile caps, rather than to help them in sustaining the superstructure load.

Therefore, this paper continues on this particular topic, exploring the numerical evaluation of standard pile groups vs. piled rafts, and the latter system advantages for real case designs. This particular exercise was incorporated as part of a jointed research project between the University of Brasília and the Czech Technical University, which has allowed one student of this latter University (first author) to develop his “sandwich” doctorate in the formerly cited institution. The data presented herein is the main outcome from this fruitful international partnership.

Thus, the main objective of the paper is to numerically analyze the behavior of small (traditional) pile groups and to compare them to the behavior of a single pile founded in an identical soil horizon. In addition, the article is also aimed at the foundation raft constructed on the top of the pile group and its influence on the overall bearing capacity, stiffness and final settlement of the overall foundation system (piled raft problem). Some attention is also paid to the distribution of the vertical reaction forces acting on the pile tip, pile shaft and top raft (in cases of piled raft systems). It is organized as follows: The introduction of the subject is followed by the review of the site’s tropical soil properties and the description of the performed field load tests. The numerical method and its application to the solved problem are also described in the second section. Further, in the results section, the numerical load-settlement curves obtained for distinct input parameters are presented and compared to existing experimental data. This set of results is followed by back calculations done with the same foundation systems and site characteristics. Finally, numerical simulations of similar systems designed with piled raft concepts are carried out, and compared to previous results in which solely traditional pile groups were simulated. Practical aspects for using numerical tools for solving problems of complex foundation systems are concluded in the final section, and the advantages of designing such systems as piled rafts are also outlined and encouraged.

2. Site and Pile Characteristics

With increasing building density in the Brazilian capital Brasília and its neighboring area (Federal district) the civil engineers have to deal with the problem of designing foundations on the tropical porous clay, which, by the way,

is commonly found throughout the Central Plateau of Brazil. This material can be geologically classified as weathered latosol of the tertiary and quaternary age. The latosol has been extensively subjected to a laterization and leaching process during the rainy seasons causing its high porosity. Throughout the district, the thickness of the latosol varies from few centimeters to more than 40 m. The clay mineral kaolinite, and oxides and hydroxides of iron and aluminum predominate in this reddish tropical soil. The variability of the properties of the Brazilian clay depends on several local factors such as topography, the vegetal cover or the parent rock (Cunha *et al.*, 1999).

Due to the leaching process and weathering, the tropical porous clay shows low unit weight and high void ratio. This properties result in the tendency of the soil to fail not only under shear loading but also by volumetric collapse. Such a presumption is confirmed by the extreme values of the coefficient of collapse which can reach up to around +12%. At the UnB experimental site, the latosol overlays saprolitic/residual soil with a significant anisotropic mechanical property and a high (SPT) penetration resistance. This underlying soil originates from a weathered, folded and foliate slate, a typical parent rock of the region. The material in the surficial layer is locally known as the Brasília “porous” clay, being geotechnically classified as sandy clay with traces of silt. All material data presented in this article refer to the geotechnical experimental research Foundation and *In situ* Investigation site of the Univ. of Brasília. The location of UnB campus within Brasilia city together with the location of the UnB experimental site is shown in Fig. 1. General soil characteristics and parameters of the soil at UnB experimental site obtained in previous research (Cunha *et al.*, 1999) are listed in Table 1.

The provided geotechnical parameters were obtained in a comprehensive laboratory and in-situ testing project carried out as a part of the postgraduate research program at UnB. Conventional classification was performed together with more sophisticated laboratory tests such as double oedometer and collapse tests, triaxial K_0 and triaxial CK_0D tests, permeability tests and direct shear tests with samples

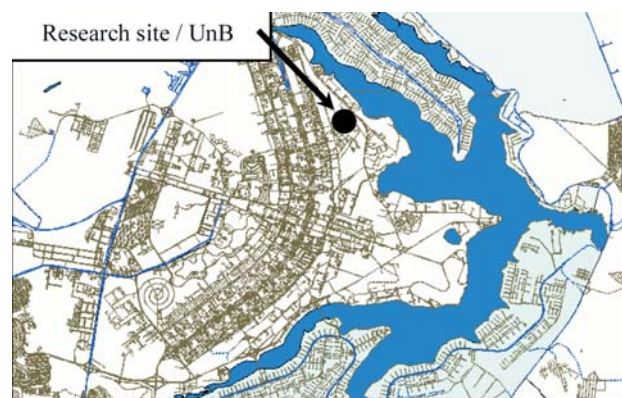


Figure 1 - Location of the University of Brasilia and UnB experimental geotechnical site.

Table 1 - General geotechnical properties of porous clay found at UnB experimental site (Cunha *et al.*, 1999).

Parameter	Unit	Range of values
Sand percentage	%	12-27
Silt percentage	%	8-36
Clay percentage	%	37-80
Dry unit weight	kN/m ³	10-17
Natural unit weight (γ_n)	kN/m ³	17-19
Moisture content	%	20-34
Degree of saturation	%	50-86
Void ratio	-	1.0-2.0
Liquid limit	%	25-78
Plastic limit	%	20-34
Plasticity index	%	5-44
Drained cohesion (c)	kPa	10-34
Drained friction angle (ϕ)	°	26-34
Young's modulus (E)	MPa	1-8
Coefficient of collapse	%	0-12
Coefficient of earth pressure	-	0.44-0.54
Coefficient of permeability	m/s	10 ⁻⁸ -10 ⁻⁵
Poisson's ratio (estimation)	-	0.2-0.35

under distinct orientations. The geotechnical profile of the UnB experimental site has been examined by a number of researchers and recently described by Mota (2003) and Anjos (2006) to name a few. Authors characterize the profile of UnB experimental site and provide material parameters for the Mohr-Coulomb model.

The design parameters were obtained in different ways. Mota (2003) used a combination of parameters obtained in laboratory (triaxial and direct shear tests) and *in situ* tests (dilatometer and cone penetration tests). See Table 2 with the UnB experimental site profile details consisting of five layers up to the depth of 15 m where the stiff bedrock is found. Since the utilization of strain sensor along the pile reinforcement provided the distribution of shear stress acting on the pile shaft it was also possible by this author to identify distinct soil layers and to determine their approximate material properties. Parameters in the geotechnical profile published by Anjos (2006) were obtained via back calculation analysis with the results from an isolated bored pile field loaded in the UnB experimental site. This backward analysis was performed with the Geo4 foundation software (Fine, 2007), which is based on a semi-analytic method as described in Anjos *et al.* (2006). The resulting geotechnical profile is shown in Table 3, based on a layering sequence defined with local experience plus the results of cone penetration tests in this same site.

Three field load tests of deep foundations constructed at the UnB experimental site are analyzed in this study. The

Table 2 - Geotechnical profile deduced from laboratory and *in situ* tests (Mota, 2003).

Layer	Depth (m)	γ_n (kN/m ³)	E (kPa)	ν (-)	c (kPa)	ϕ (°)
I	0-3	14.0	900.0	0.2	10.0	27.0
II	3-6	15.0	2200.0	0.2	10.0	27.0
III	6-9	16.0	7300.0	0.2	25.0	27.0
IV	9-12	17.5	10000.0	0.2	40.0	27.0
V	12-15	19.0	10000.0	0.2	40.0	27.0

ν = Poisson's ratio.

Table 3 - Geotechnical profile obtained via backward analysis performed in FINE Geo4 (Anjos 2006).

Layer	Depth (m)	γ_n (kN/m ³)	E (MPa)	ν (-)	c (kPa)	ϕ (°)
I	0-2	13.5	23	0.29	4	36.6
II	2-6	14.4	20	0.33	10	29.8
III	6-8	15.0	22	0.32	9	31.4
IV	8-9	18.0	23	0.31	7	33.1
V	9-12	17.8	24	0.31	7	33.2
VI	12-15	18.5	35	0.28	3	37.1

single pile test, the group of two piles and the group of three piles are labeled as EHC1, EHC2 and EHC3, respectively in accordance with Anjos (2006) nomenclature. The Continuous Flight Auger technology was adopted to construct the piles and no injection pressure was used during the construction phase, given very soft characteristics of the surficial clay of the experimental site. Hence, during the last construction phase the auger was gradually removed with simultaneous casting of concrete under only atmospheric pressure. Although this technical simplification may cause decrease in the final bearing capacity of the entire foundation system, it allows for a straightforward numerical analysis which is also applicable to traditional bored piles. The arrangement of piles within the UnB experimental site is shown in Fig. 2 together with other tested piles and *in situ* tests carried out there by this as well as previous studies. Figure 3 shows the CFA drilling machine used to bore and cast the piles.

All piles used in the tested foundations were built with the same dimensions. The nominal diameter was 0.3 m and the nominal length 8.0 m. In the case of the pile groups EHC2 and EHC3 the axial distance between the piles was 0.9 m. The top three meters of all piles were reinforced with four steel bars with 16 mm diameter and 6.3 mm stirrups with distance of 0.15 m. A concrete block without physical contact with the underlying soil was constructed on the top of the EHC1 single pile as well as on top of EHC2 and EHC3 pile groups. See photos in Figs. 4 and 5.

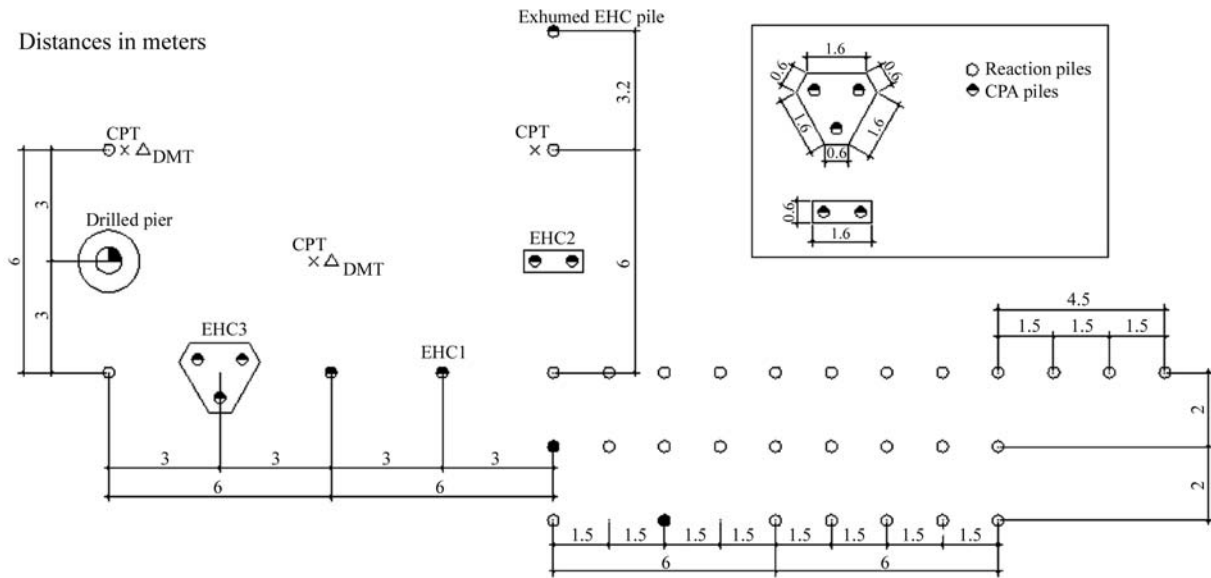


Figure 2 - Plan of UnB experimental geotechnical site (after Anjos, 2006).



Figure 3 - CFA drilling machine.

Apart from the six piles used for load tests, a testing pile of 2.8 m length was also constructed. Later, this pile was exhumed to give a general idea about how the real pile geometry differs from the nominal values. The real diameter of the testing pile varied from minimal value 0.280 m to maximum 0.360 m with the mean of 0.303 m. Although there was evident increase of diameter closer to the base, the mean diameter did not differ significantly from the nominal value of 0.3 m. The location of the exhumed pile is presented in Fig. 2 and the real geometry of it is visible in Fig. 6. All foundations were constructed in the rainy season of Brasília city (October to March) while the load tests were carried out in April, which follows dry season months.

3. Numerical Finite Element Analyses

Since a 3D effect is essential to understand the pile-soil interaction, the software Plaxis 3D Foundation was used in the numerical analysis. This software is based on

displacement based finite element method (Plaxis 2007) and allows for using standard geotechnical material models based on the theory of plasticity. The outcome of the analysis is graphically represented by the distribution of displacements, strains and stresses or the load-settlement curve.

3.1. Geometrical model

The geometrical model described below adopted dimensions of each tested foundation. In the horizontal layout, the analyzed area was a 12 m x 12 m square with the foundation system in the middle. Equally to the real experimental foundations, the top raft in the geometrical model was separated from the surrounding lateral surface by a narrow gap as plotted in Fig. 7.

In Plaxis 3D Foundation the vertical layout of the construction is determined by horizontal planes also called working planes. Two main working planes at ± 0 m and -15 m levels form the surface and bedrock levels, creating the vertical boundaries of the analyzed area. Another vertical plane bounds the bottom of the floating piles at -8.6 m. Two additional working planes were added to create the bottom surface of the surficial raft (-0.4 m) and the bottom of the excavation under the surficial raft (-0.6 m). This pair of working planes allowed to create free space under the raft as plotted in Fig. 8 (a), exactly as field loaded by Anjos (2006).

Once the geometry of the traditional pile group was created, it could be easily changed in order to simulate the response of a piled raft system which could be constructed in contact with the subsoil. This was achieved by assigning the soil to the region below the top raft of the pile groups. The difference in the geometry of the piled raft and the pile

group can be respectively noticed by comparing Figs. 8b and a.

3.2. Material model

The majority of the computations were carried out using the Mohr-Coulomb failure criterion as a material model for the soil. This standard model for soil materials exhibits linear behavior followed by a perfectly plastic response after the plasticity condition is reached. No hardening or softening of the material was assumed. Besides the Mohr-Coulomb there is also the so called Hardening Soil model which allows increasing the failure stress according to plas-



Figure 4 - Piles of EHC1, EHC2 and EHC3 foundations before construction of the top block.

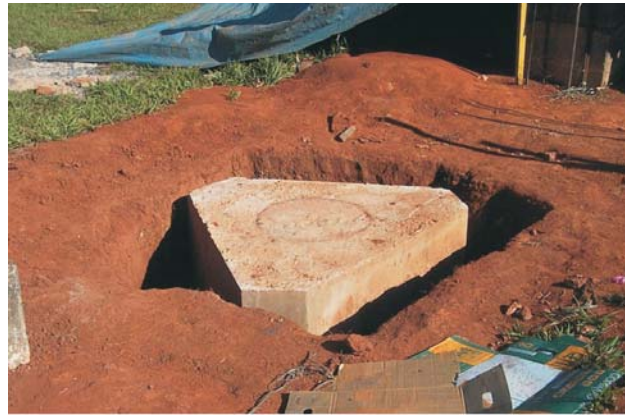


Figure 5 - Top blocks of EHC2 and EHC3 foundations.



Figure 6 - Exhumed testing CFA pile.

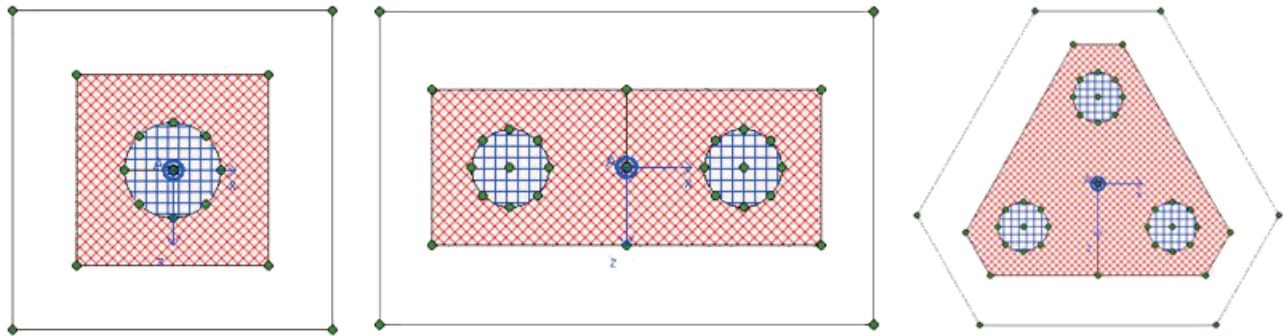


Figure 7 - Horizontal layout of EHC1, EHC2 and EHC3 models.

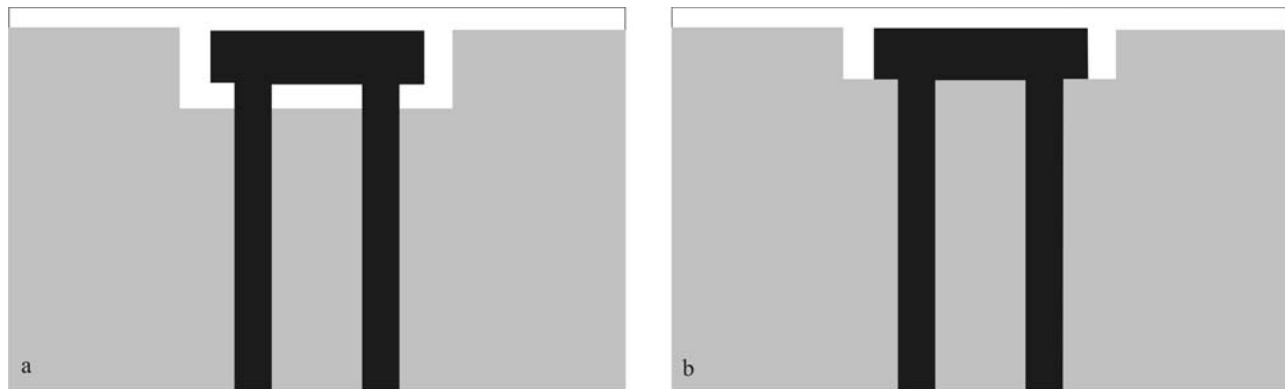


Figure 8 - Vertical layout of the geometrical model - detail of the EHC2 system.

tic shear stress. Despite the fact that such a property gives better precision to many types of soils it does not surpass the standard Mohr-Coulomb model when modeling this particular type of porous clay. The tendency of the material to collapse, *i.e.* to exhibit sudden large irreversible volumetric and shear strains, would need a material model that allows not only for strain hardening but also for strain softening. Owing to the absence of underground water in the geotechnical profile at the testing period, no pore pressure was assumed during the analysis. The soil environment was modeled by five horizontal layers when employing laboratory and *in situ* parameters (Table 2) or by six layers when using the back analyzed parameters published by Anjos (2006) (Table 3).

The concrete reinforced piles and the top rafts were modeled as homogenous nonporous linear elastic material with Young's modulus $E = 20$ GPa, Poisson's ratio $\nu = 0.2$ and a unit weight $\gamma = 24$ kN/m³. Although in the real construction the top part of the pile, together with the top raft, was reinforced with projecting bars and stirrups, no additional reinforcement was incorporated in the numerical model.

3.3. Finite element mesh

An automatic mesh generator built in Plaxis 3D Foundation code was used to create the three-dimensional

finite element mesh. The 3D mesh was generated in two steps. In the first step, the two dimensional mesh consisting of six node triangular elements was automatically created. The triangular mesh was then refined in the area surrounding the pile in order to eliminate long narrow triangles which the generator produced in this region. See the refined 2D mesh in Fig. 9. The global mesh refinement was not used in the analysis since it does not influence the resulting load-settlement curve but, as proved in a benchmark test, consumes more computation time. In the second step, this 2D triangular mesh was extended into 3D mesh compounded of 15-node wedge elements with two horizontal triangular faces and three vertical rectangular faces. In this type of three dimensional elements, three nodes are found along each edge allowing for quadratic approximation of displacement field within the volume of the element.

A relative vertical displacement along the interface between the pile shaft and the surrounding soil was allowed by means of interface elements. Hence, 16-node interface elements of zero thickness were inserted along the contact between wedge elements representing the solid construction and wedge elements representing the surrounding soil. The mechanical properties of these elements were derived from the material parameters of the neighboring soil. Thus, in the solved problem, the interface elements also followed Mohr-Coulomb failure criterion deriving the ultimate shear

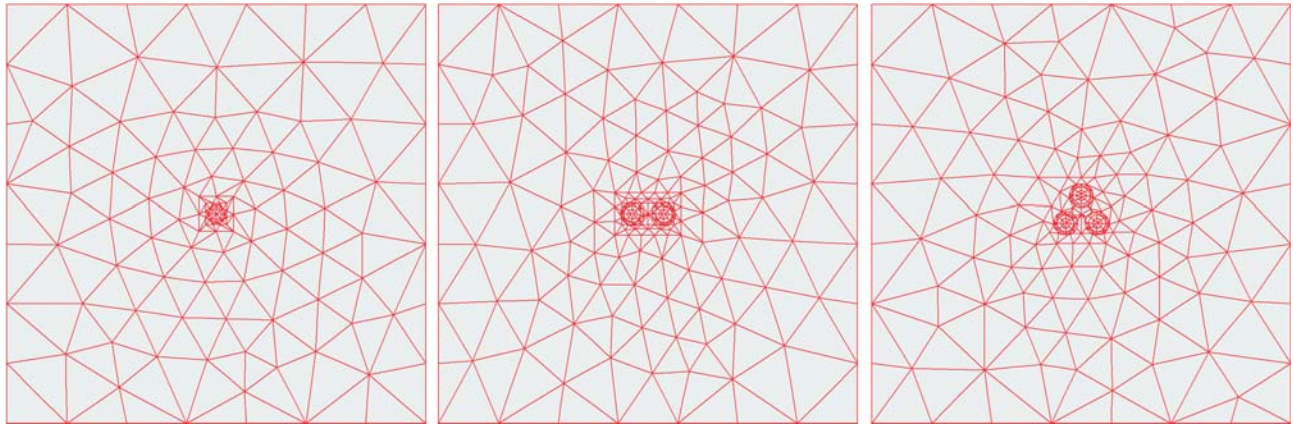


Figure 9 - 2D triangular finite element mesh extended to 3D wedge elements.

stress from the actual normal stress acting perpendicularly to the pile shaft.

3.4. Computation stages

The computation stages were defined in order to follow the phases of construction of the foundation system and the load test itself. In each computation stage the system was loaded with self weight and, if present, external forces. Subsequently, the incremental solver built in Plaxis was used to compute the changes in displacements and stresses. The problem of the field load test was modeled in the following four stages:

- Initial stage - The initial stress state of the soil before construction is created in the initial stage. The initial stage is often referred to as K_0 -procedure. The displacements are set to zero after this initial phase;
- Construction stage - During the second stage a small excavation on the surface is created and the entire foundation system (pile with the concrete raft on the top) is constructed;
- Loading stage - The third stage is the loading stage. The geometry of the model is inherited from the second stage and the vertical load is applied. Data of the loading branch of the load-settlement curve are obtained in this stage;
- Unloading stage - The last fourth stage refers to the unloading. The geometry and materials are the same as in the loading stage, only the vertical load is removed. The unloading branch is computed in this last phase.

Only the original soil at natural water content is found in the geotechnical profile during the initial stages. Conventionally, the vertical stress along the depth is in the unsaturated condition, computed by using the natural specific bulk weight of the soil.

A simple relationship in the form

$$\sigma'_v = \gamma_n h \quad (1)$$

was used to generate the initial vertical stress in the soil. The symbols σ'_v , h and γ_n respectively denote effective ver-

tical stress, depth and natural unit weight of the soil. The effective horizontal stress σ'_h then follows from:

$$\sigma'_h = K_0 \sigma'_v \quad (2)$$

where K_0 is the coefficient of earth pressure at rest computed using constant value of Poisson's ratio:

$$K_0 = \frac{\nu}{1-\nu} \quad (3)$$

For the present values of ν , the coefficient of earth pressure varied in the range 0.25-0.5, which reasonably agrees with *in situ* test measurements at the UnB experimental site (Table 1).

In the second computational stage the soil material is replaced with elastic material in order to model the concrete piles and the concrete raft on the top. The soil surrounding the raft is also excavated. The forces acting in the system refer only to loading or unloading caused by changes in the unit weight of the newly introduced materials, or by the excavation. No additional external load is added to the system in this stage.

The main computations which provide the load-settlement curves are carried out in the third stage. Here the vertical load is applied on top of the raft, and the loading branch of the load-settlement curve of a previously chosen monitoring point is computed. In all models the monitoring point was placed in the middle and on the top of the raft.

In Plaxis 3D Foundation software, the entire load defined at the beginning of the computation stage is automatically divided into load increments. The size of the increments respects the degree of nonlinear behavior. Generally spoken, the increments size decreases when the plastic zone in the pile neighborhood propagates but it remains quite large during elastic response. In the presented computations the entire applied load varied with each solved problem, as shown in Table 4. These particular values of the vertical load allowed for reaching full mobilization of the piles until the onset of the foundation failure. On the other hand, such values of the load are small enough to reach equilibrium at the end of each loading stage, and do not cause nu-

Table 4 - Values of vertical loading used in the numerical analyses (kN).

Loading case	EHC1	EHC2	EHC3
Laboratory and <i>in situ</i> parameters	300	600	900
Back analyzed profile (Geo4)	300	600	900
Pile group	400	800	1200
Piled raft	600	1200	1800
Analyses before failure	200	400	600

merical instability during computations. The differences in the load levels presented in Table 4 also reflect the different bearing capacity and settlement of the distinct foundations systems and analyzed geotechnical profiles, in order to reasonably draw both the elastic pre-failure and elasto-plastic post-failure branches of the particular load settlement curves.

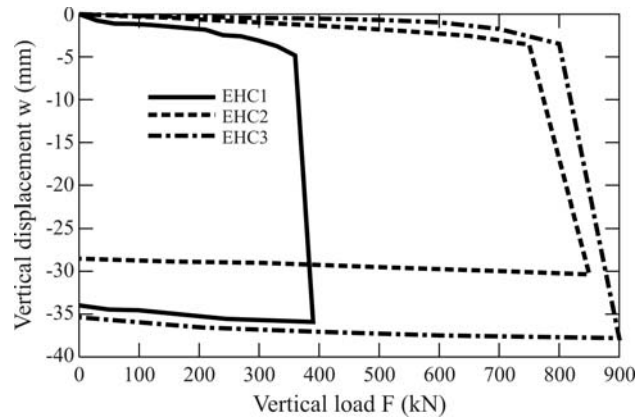
The last stage (fourth) corresponds to unloading. The load added in the previous computational stage (third) is removed and the foundation heaves. Similarly as in the previous stage, the load is removed in several steps allowing the unloading branch of the load settlement curve to be plotted. The same monitoring point on the top of the foundation systems was used here. Unlike the loading stage, no significant plastic deformation usually occurs during unloading, and the automatically determined load steps are larger.

As mentioned before, the behavior within particular loading/unloading stages is examined by using the so called monitoring points. If a monitoring point is defined prior to the computational stage, the load scaling factor, and corresponding displacement of that point for each loading step is stored and can be displayed within "Plaxis Curves" module, or simply exported as a list of data to form the load-settlement curve.

4. Experimental Data and Discussion of the Numerical Results

4.1. Experimental results

The experimental results from the pile load tests EHC1, 2 and 3 are presented in Fig. 10. From this one, it is evident that the load-settlement curves present an initial stiff and relatively linear response, beyond which all curves fail abruptly due to uncontrolled measured settlements. The linear branch reaches the failure point which is at the level of 360 kN of vertical load for EHC1, 700 kN for EHC2 and 800 kN for EHC3. The vertical settlement measured prior to the failure reached 4.8 mm, 3.6 mm and 3.5 mm for EHC1, EHC2 and EHC3 respectively. After increasing the vertical load to 390 kN (EHC1), 850 kN (EHC2) and 900 kN (EHC3), hence by approximately 8%, the foundations showed large irreversible settlements reaching respective values of 35.9 mm, 30.4 mm and 37.8 mm. The unloading branch of the load-settlement curve was mea-

**Figure 10** - Experimental results from the pile load tests carried out on EHC1, EHC2 and EHC3 foundations (after Anjos, 2006).

sured from these final points, as shown in this same figure. The unloading branches of the load-settlement curves are relatively parallel to the initial (elastic) branches of the loading curves, preserving a close to irreversible settlement constant.

It is obvious from the results that the sudden failure, accompanied by a rapid increase of the settlement of the system, was caused by a collapse of the soil around the foundation elements, given the well known collapsibility and meta-stable structure of the porous clay of Brasília. Nevertheless, even with these particular features, the experimental curves were used to be compared to numerical simulations of all pile group systems with Plaxis 3D Foundation software. After all, the analyses must refer to a realistic foundation behavior in this particular tropical clay, by using loaded systems as close as possible to normal field conditions.

4.2. Numerical results

4.2.1. Results obtained using laboratory and *in situ* parameters as input

The first numerical simulation was carried out with a set of parameters obtained via laboratory and *in situ* tests, as interpreted by Mota (2003) and stored in Table 2. The resulting load-settlement curves computed in loading and unloading stages are displayed in Fig. 11. It is evident from this figure that the computed failure level, *i.e.* the load level by which the settlement rate starts to increase and the loading branch starts to bend down, reaches only approximately 60% of the measured failure load in the case of EHC1 and EHC2 and about 80% for EHC3. It should also be remarked that the differences in the initial numerically derived stiffnesses of the foundations systems are even more visible. It was also observed that the numerical displacements, at failure level, varied from 20 mm (EHC1) to 30 mm (EHC3), while the measured displacements before failure point were in the range of about 4 mm. Besides, regardless of the inaccuracies when using this set of parameters

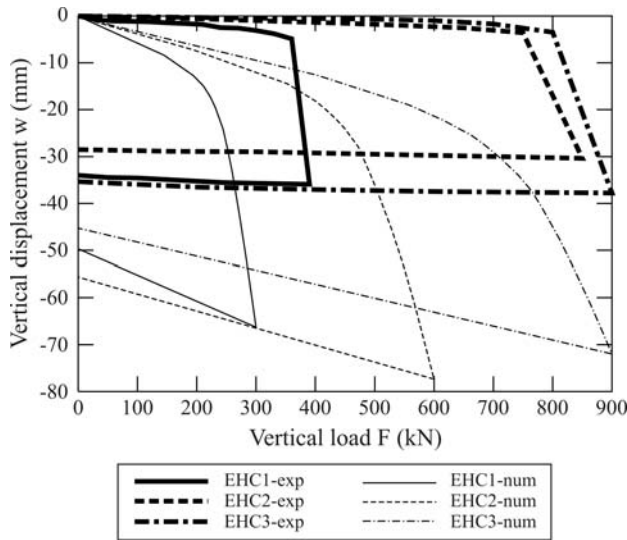


Figure 11 - Measured load-settlement curves and numerical results obtained for material parameters from laboratory and *in situ* tests (data from Mota, 2003).

(Table 2), the adopted model generates irreversible settlements which remain approximately constant during the unloading stage.

It follows from the present series of analyses that, to properly simulate pile load experiments on isolated or traditional pile groups founded on this particular soil, it does not seem to be possible to directly use geotechnical parameters deduced from conventional laboratory or *in situ* tests, as those presented in Table 2 for the UnB experimental site. Perhaps, either the modeling technique is not appropriate to capture the detailed nuances of the real site phenomenon, or the used parameters do not properly represent system interactions (foundations/soil/external factors) that take place during pile construction and loading, or both cases hinder the analyses simultaneously.

As examples of neglected aspects (in the present numerical analyses) that may have influenced the group behavior in such soil, one can mention the suction variations of the subsoil, the complex interactions between foundation elements and the surrounding soil, the minor changes or variability of construction techniques from pile to pile, the distinct technological influences on the surrounding soil by pile excavation and casting at distinct dates, the different and unknown stress paths along soil elements surrounding the foundation systems, the complex stress strain curves of heterogeneous soil elements around the piles, and so on.

Finally, underestimated foundation stiffness as observed for computations using the combination of laboratory and *in situ* material parameters can also be caused by the differences in the secant Young modulus E_{50} of the measurements and the elastic Young modulus E^{el} used in the Mohr-Coulomb material model. The choice of the unloading-reloading Young modulus E_{ur} would be perhaps more appropriate here, but such experimental value has not been

determined with the available triaxial experiments of this porous clay.

4.2.2. Results obtained by the use of parameters via FINE Geo4

Given the aforementioned results, another series of analyses were carried out by employing back analyzed results via another numerical (Geo4) technique, as published by Anjos (2006) and summarized in Table 3. It is again noticed that the back analyzed parameters of this author were obtained for an isolated bored pile, rather than a pile group.

The result of this new analysis is presented in Fig. 12 where it is observed that a slightly better and closer agreement between simulated and measured curves is achieved, although still not a perfect match. Nevertheless, similarly as the previous case, with the idealized adopted geotechnical profile of Anjos (2006) it is noticed that the numerical analyses lead again to underestimated bearing capacity values. On the other hand, some improvement can be noticed in the initial part of the loading branch, suggesting a perhaps more realistic macroscopic stiffness of the foundation system than those generated for the previously adopted (idealized) geotechnical profile. However, in spite of the improvement, the stiffness before failure for all simulated systems is still underestimated.

It follows again that simulation of the pile groups founded in this particular subsoil should be better conditioned, as a proper solution could still not be addressed by adopting back calculated parameters from a previous series of analyses. It is indeed questionable if parameters derived from a slightly distinct numerical technique would be useful to simulate a system under the framework of another, more complex, modeling tool. It was expected that both methods would give comparable results when using the

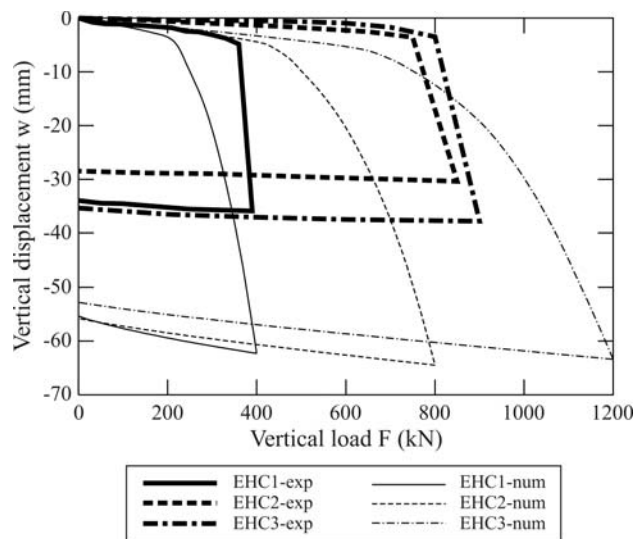


Figure 12 - Measured load-settlement curves and numerical results obtained for material parameters from backward analysis with Geo4 software (data from Anjos, 2006).

same Mohr-Coulomb material model, but this hasn't been exactly the case observed with the results.

4.2.3. Results obtained from backward calculation analysis of EHC1 single pile

The previous items demonstrated that the numerical results failed to meet the experimentally obtained load-settlement curves with sufficient engineering accuracy, either by employing parameters obtained on a combination of laboratory and *in situ* tests or by employing values from a backward calculation of a single pile with another numerical tool. Hence, in order to reach an even better agreement, a backward analysis of the EHC1 single pile was performed in Plaxis 3D Foundation, the same software adopted to simulate all other pile group systems.

In this analysis a homogeneous subsoil profile was assumed, while the predetermined geometry of a single pile EHC1 was kept unchanged. The parameters of the unique material which forms the entire soil horizon were varied using a simple trial and error method. Only a selected set of material parameters was changed during the backward analysis. In particular, it was decided to vary the elastic Young modulus, the friction angle and the cohesion while the unit weight, the Poisson's ratio and the dilation angle were kept constant. The elastic parameters of the concrete forming both pile and raft elements were also excluded from the backward analysis, and kept constant. Moreover, it was realized during the trial and error computations that the presence of the interface elements is absolutely essential for reaching the sudden collapse of the foundation system, as experimentally observed in the field.

The resulting values are presented in Table 5, while the best fitted load-settlement curve is displayed in Fig. 13. As expected, the best agreement with the measured data was provided by the computations when the back analyzed parameters were derived from the EHC1 single pile test. Both the pre-failure stiffness and the bearing capacity simulated for the single EHC1 pile exhibited a close approximation to the experimental values, validating the use of parameters presented in Table 5 for the other foundation systems. Figure 13, in addition, shows how the load-settlement curve changes when a thin layer of soil is removed from under the pile tip. In spite of that, the system with no tip resistance fails at a load level lower by only 8% than the critical failure point. Up to this stage, both back analyzed curves, with and without tip resistance, are quite identical,

Table 5 - Results of backward analysis performed on EHC1 single pile with Plaxis 3D.

γ_n (kN/m ³)	E (MPa)	ν (-)	c (kPa)	ϕ (°)	ψ (°)
18.0	35.0	0.3	32.0	27.0	0
Assumed	B.a.	Assumed	B.a.	B.a.	Assumed

Ψ = dilation angle. B.a. = Back analyzed.

which indicates the predominant contribution of the shaft friction to the total capacity of a single pile in such a geotechnical profile. Indeed, such conclusion has already been experimentally shown before by Mota's (2003) instrumented pile load test results at this same site.

4.3. Numerical results of the other systems

The resulting load-settlement curves of all EHC foundations computed with the back analyzed material parameters from Table 5 are plotted in Fig. 14. The curves were also derived by considering interface elements around the piles and soil underneath their tips. It is clearly noticeable a much better agreement between measured and computed curves for the single (EHC1) as well as the group of two piles (EHC2). The average difference in the failure load for these previous cases is less than 5%, while the computed displacements before failure are approximately 25% higher than the measured values. Besides, the adopted model was

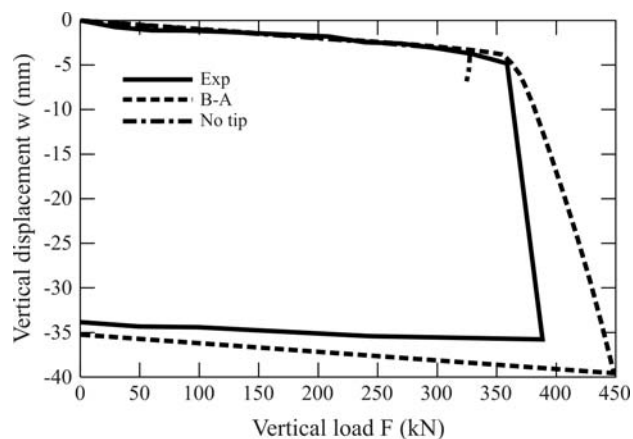


Figure 13 - Results of backward analysis on single CFA pile EHC1 performed in Plaxis 3D.

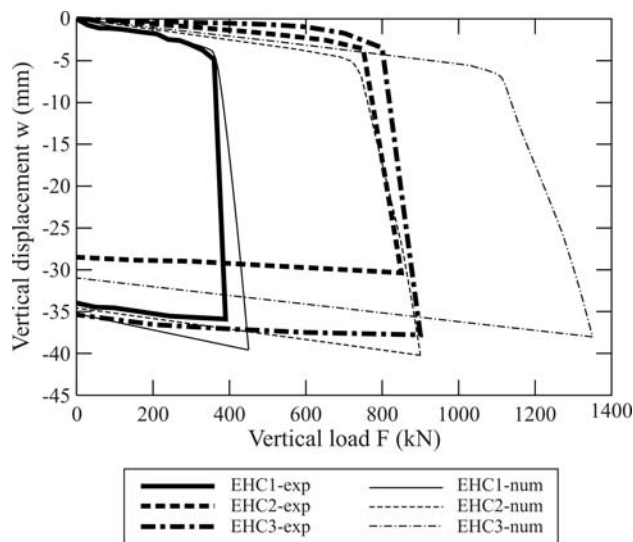


Figure 14 - Experimental and numerical load-settlement curves, using back analyzed parameters in Plaxis 3D.

also able to simulate the sudden failure with rapidly increasing irreversible settlements occurring with small load increments.

Mutual comparison of computed results obtained numerically for EHC1, EHC2 and EHC3 pile group systems also lead to the observation that the group effect, at least for the pile spacing adopted in the present research, slightly reduces the overall foundation stiffness, and may have somehow a small influence on the bearing capacity.

Nevertheless, a large difference was found between numerical and experimental results for the third, EHC3 pile group. As one may infer from Fig. 14, this particular group did not follow a predicted pattern as would be expected solely by the EHC1 and EHC2 results. For instance, Anjos (2006) results, graphically expressed in Fig. 10, indicate that the vertical loading stage just before the sudden failure was 360 kN (at 4.85 mm top displacement), 750 kN (at 3.57 mm) and 800 kN (at 3.47 mm) respectively for EHC1, 2 and 3 systems. Adopting as reference the load for the isolated pile EHC1, these numbers represent an increase of approximately 2.1 and 2.2 times respectively for EHC2 and 3 systems. Slightly differences can be found, given distinct displacement levels upon which the load values are taken, but, nevertheless, one can argue if the load obtained for the EHC3 system was indeed in the correct range it would be normally expected. According to Anjos (2006), for this particular system it was possible to estimate an efficiency factor of around 0.8 by standard empirical relationships used for floating piles in clay. This number seems to be close to the experimental measured efficiency of around 0.74, but, again, one may argue about its correctness. Actually, if the EHC3 group was submitted to the influence of pile to pile interference, which would justify the decrease in load efficiency, the same behavior would also be expected in the EHC2 system. Based on the limited available data, the authors' opinion is that only an efficiency reduction can not explain the discrepancy between EHC3 and EHC1 results. Hence, having said that, it will be assumed from this point on that the experimental results from the EHC3 system may be compromised, therefore not serving to conclude on the appropriateness of the numerical simulations of the EHC3 load-settlement curve.

4.4. Pile group vs. piled raft

Having the material model calibrated it was decided to examine how could the raft, in full contact with the surficial soil, positively contribute to the mechanical response of the entire foundation system for each of the studied cases. Off course, given the fact that no experimental site tests were carried out with the top raft in active contact with the soil, this subsection will entirely rely on numerical simulations of the systems. It will be assumed that the numerical load-settlement curves presented in Fig. 14, for all systems, are appropriate in engineering terms and can reasonably serve as benchmark for comparison purposes with

equivalent curves from numerically derived "piled raft" simulations.

Thus, by activating the soil layer beneath the top raft, as exemplified in Fig. 8 (b), it was possible to obtain piled raft related load-settlement curves, and to compare them directly with the numerical ones from the pile groups of Fig. 14. Such comparison is depicted in Fig. 15 where it is noticed that the ultimate bearing capacity was increased by 17% for EHC1, by 12% for EHC2 and by 15% in the case of EHC3, when considering the piled raft configuration. The settlement during the initial (elastic) phase, for the all piled raft cases, shows an average slightly smaller value, decreased by approximately 7% to that equivalent of the pile group cases.

The slightly increased stiffness in the initial phase of the load-settlement curve of the piled raft systems, in comparison to the standard pile groups, is visible in Fig. 16. This figure presents a zoom of the initial part of the curves depicted in Fig. 15.

Finally, one of the most visible contributions of the foundation behavior as a piled raft is the softening of the abrupt plastic failure which has been exhibited in the simulated curves of the pile group systems. This is valid for all studied cases. Indeed, the failure of the piled raft foundations is markedly more gradual as the load is constantly shared by two elements of distinct behavior: raft and pile, plus surrounding soil. For instance, the raft has an increasing load capacity with settlement, and the pile has a limited value of shaft load capacity, which is mobilized at a low displacement range. This is combined to an increasing load capacity at tip, which generally also increases with higher displacement.

4.5. Load shared by pile shaft, pile tip and raft

The distribution of the internal forces acting in the pile element provides information about the percentage of

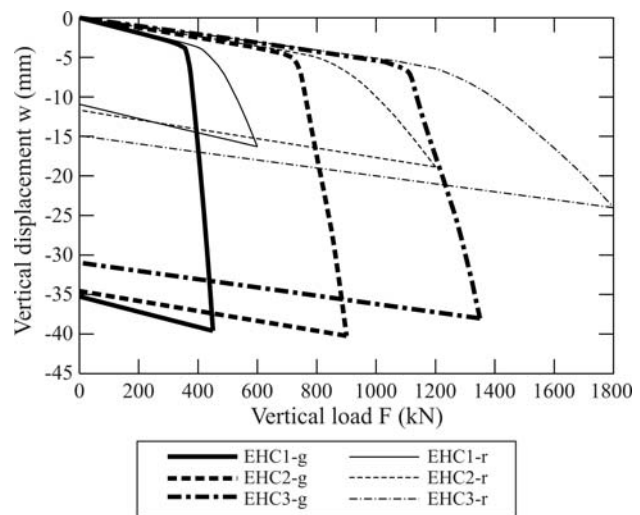


Figure 15 - Differences in the load-settlement curves numerically derived for pile groups (g) and piled rafts (r) with Plaxis 3D.

load which is attributed to the pile tip, pile shaft and possibly the raft. The distribution of the internal forces was derived from the pattern of vertical stresses displayed in the Plaxis Output module. Such a result, for illustration purposes only, is presented in Fig. 17, and has been used to determine the percentage of structural load mobilized along each of the piles of the analyzed systems.

Two sets of computations were performed in this study. The first set simulated the state of load distribution just prior to the failure, while the second examined the load distribution in already failed systems. Hence, the data as post failure refer to the state at the end of third computa-

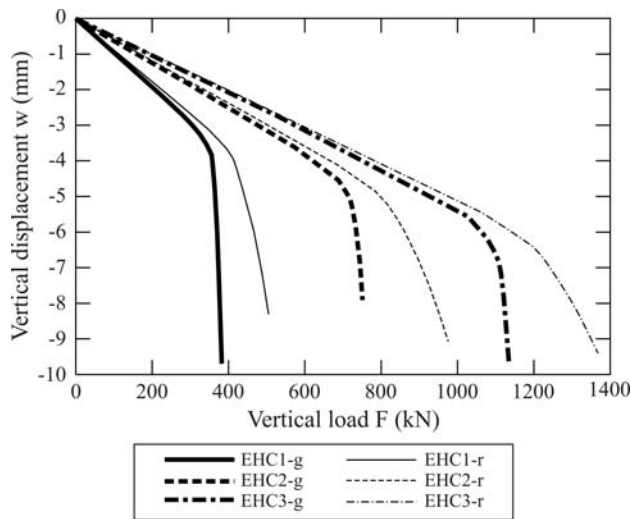


Figure 16 - Differences in the load-settlement curves numerically derived for pile groups (g) and piled rafts (r) - Zoom of initial loading stage.

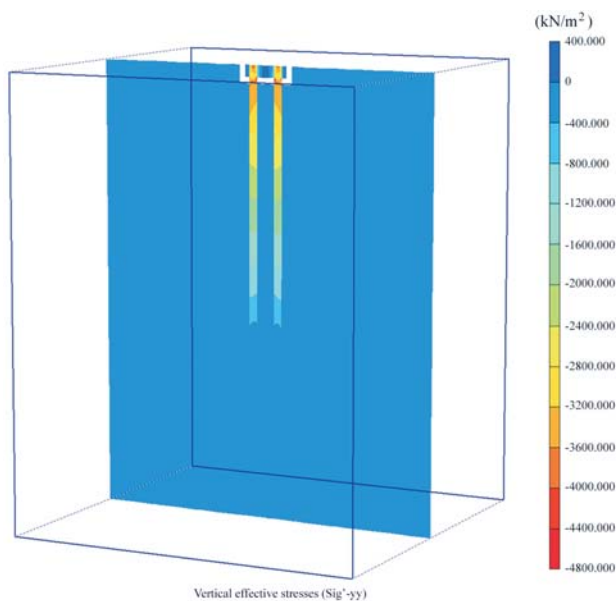


Figure 17 - Illustrative example of the output of the vertical stress distribution in the pile.

tion stage, *i.e.* after the whole vertical loading has been applied. It corresponds to the end point of the load-settlement curves in Fig. 15. On the other hand, the data denoted as pre-failure refer to analyses in which the system was loaded with 200 kN, 400 kN and 600 kN for EHC1, EHC2 and EHC3 respectively. It can be seen in Fig. 15 that such values of the external load do not cause significant settlement and can be referred to as pre-failure state. The distribution of the vertical internal load for the state before failure is shown in Figs. 18 (a) and (b). Figure 18a shows the results for pile groups EHC1, EHC2 and EHC3 while Fig. 18 (b) provides the load distribution for the piled raft systems. The values expressed for the systems EHC2 and 3 represent the average load computed for all the piles, in all cases.

The results of this figure indicate that, for the pile group, 8% of the load is carried by the pile tip while the remaining 92% of the total load is carried by the pile shaft, as already expected, given aforementioned observations of the large contribution of the shaft friction to the total pile capacity. Indeed, the piles within the studied pile groups behaved more as floating elements than end bearing ones. The same trend was noticed for the case of the piled raft systems, with average results of 7% of the total load carried by the pile tip and 83% for the pile shaft. However, in the piled raft cases, an average value of 10% of the total applied load was absorbed by the raft.

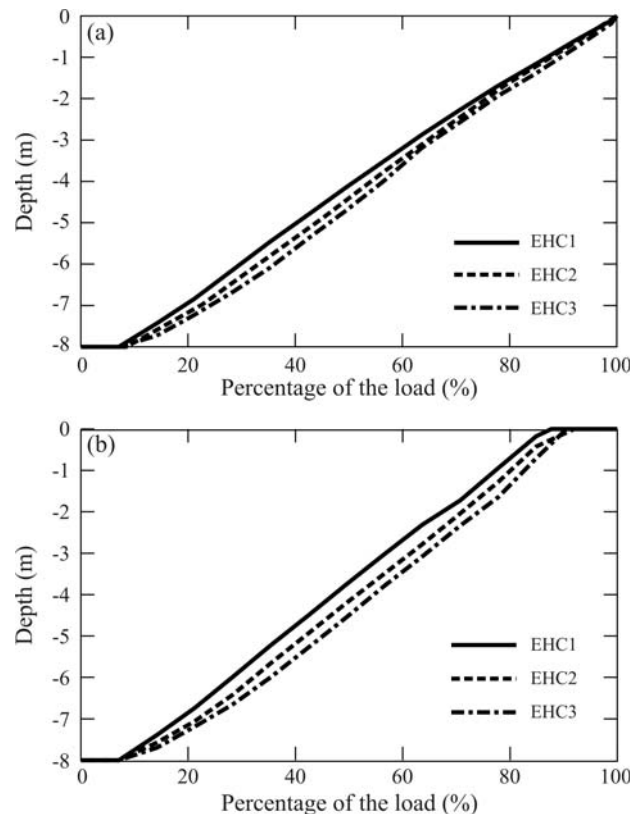


Figure 18 - Internal load distribution along the pile - stress state before failure, (a) pile group, (b) piled raft.

The distribution of the vertical internal load for the state after failure is shown in Figs. 19 (a) and (b), similarly as the previous figures. It is noticed with the results at a post failure event, for both studied systems, that the load distribution pattern did not change considerably as in the previous case. However, the magnitude of the load share has slightly shifted upwards. For instance, for the pile group 21% of the load is carried by the pile tip while the remaining 79% of the total load is carried by the pile shaft, thus giving a better end bearing performance for the piles. In the case of the piled raft systems, an average result of 11% of the total load was carried by the pile tip, 63% by the pile shaft, and 26% of the load was absorbed by the raft.

This subsection allowed the perception of the distinctive behavior of both pile group and piled raft systems when loaded at working and at failure levels. For the particular studied case, and taking on account the weak characteristics of the surficial tropical and porous Brasília clay, both systems have operated with piles with predominantly floating characteristics, where major part of the load was absorbed by lateral friction along the shaft. Nevertheless, some tip load was mobilized, respectively at ranges below 10% of the total applied load, for working levels, and beyond this range on post failure events. A beneficial absorption of the overall load by the raft, in both conditions, was clearly noticed with the piled raft systems. In working conditions, and even for low soil resistances at surface, the raft was able to

sustain 10% of the total load. In failure, the piled raft systems had the load predominantly migrated from the pile shaft to the raft, rather than to the pile tip, as previously observed for the pile group systems.

In other words, the raft aids in the overall behavior on pre and post failure events, being indeed an asset when designing the foundation as a piled raft system. However, the positive impact of the raft seemed to be more substantial when settlements higher than approximately 5 mm took place in the piled raft system. This is, off course, related to the weakness of this surficial porous clay layer, and may change to systems founded on rather more competent strata. As observed by the simulations, after this level of displacement the percentage of load carried by the pile tip and the raft increase more substantially with the amount of settlement.

4.6. Distribution of lateral friction resistance mobilized along pile shaft

Similarly as the previous analyses, and taking again on account Plaxis outputs as the one presented in Fig. 17, it was possible to determine the distribution of the lateral friction resistance mobilized on the pile shaft along its entire length. Again, the results for each of the piles from both EHC2 and 3 systems were averaged in order to be presented in the following figures.

Hence, Fig. 20 (a) and (b) respectively present the lateral shear stresses computed for the pile group and the piled raft systems for load levels just prior to failure. For both cases, average values in the range of 20 kPa to about 35 kPa were found, which agree with experimental results from Mota (2003) measured at equivalent load levels on a bored pile with similar dimensions loaded in this same site. Similarly as this experimental case, the numerical simulations have also shown that higher levels of lateral friction are mobilized closer to the pile tip than to the pile cap. Besides, the average results seem to be in the same magnitude for all studied systems, when cross comparing only the pile groups and only the piled rafts.

Nevertheless, when directly evaluating pile groups to piled rafts, one may notice that the presence of the raft has caused an increase of the level of the lateral friction in the vicinity of the raft, *i.e.*, within the pile shaft zone of up to 0.5 m underneath the raft, or ~ 1.5 diameters (d). This phenomenon becomes much more evident when comparing the results at a post failure event, as presented in Figs. 21 (a) and (b).

Again, these figures refer respectively to pile groups and piled rafts. In this case, it is noticed that the zone of increased lateral friction has extended to 0.8 m (~ 2.5 d), 2.2 m (~ 7.3 d) and 1.2 m (~ 4.3 d) underneath the raft, respectively for the EHC1, EHC2 and EHC3 piled raft systems. Indeed, there seems that the larger is the surficial area of the raft, the deeper will be the zone along the pile length affected by lateral friction increase.

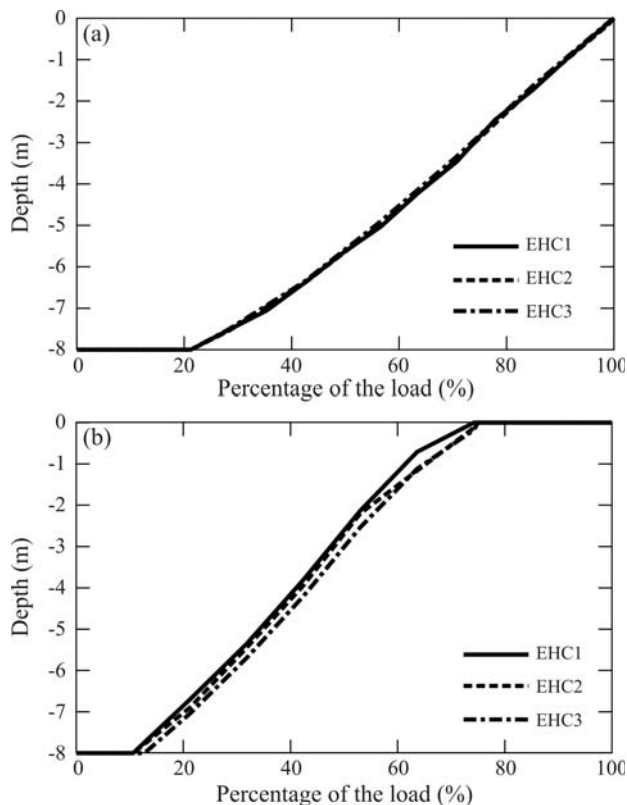


Figure 19 - Internal load distribution along the pile - stress state after failure, (a) pile group, (b) piled raft.

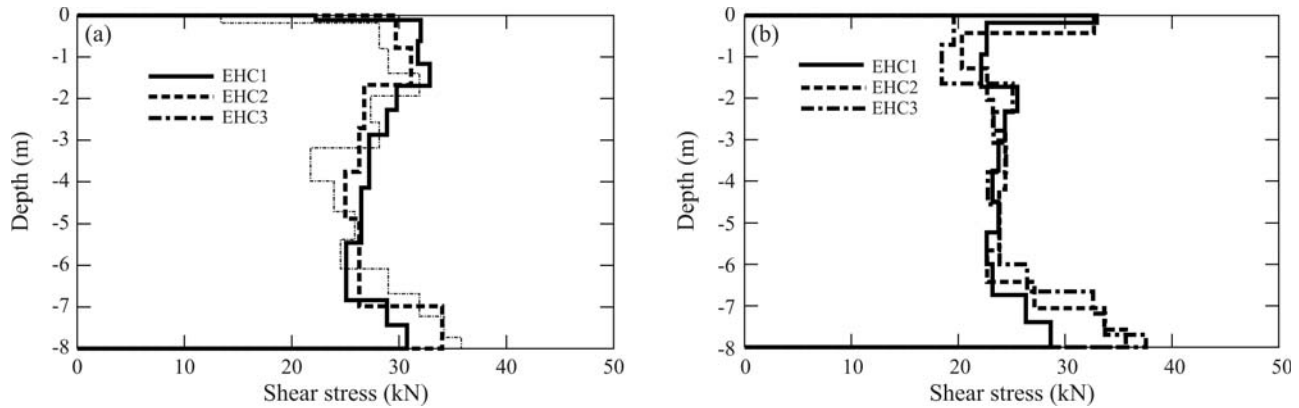


Figure 20 - Lateral friction stress distribution along the shaft - stress state before failure, (a) pile group, (b) piled raft.

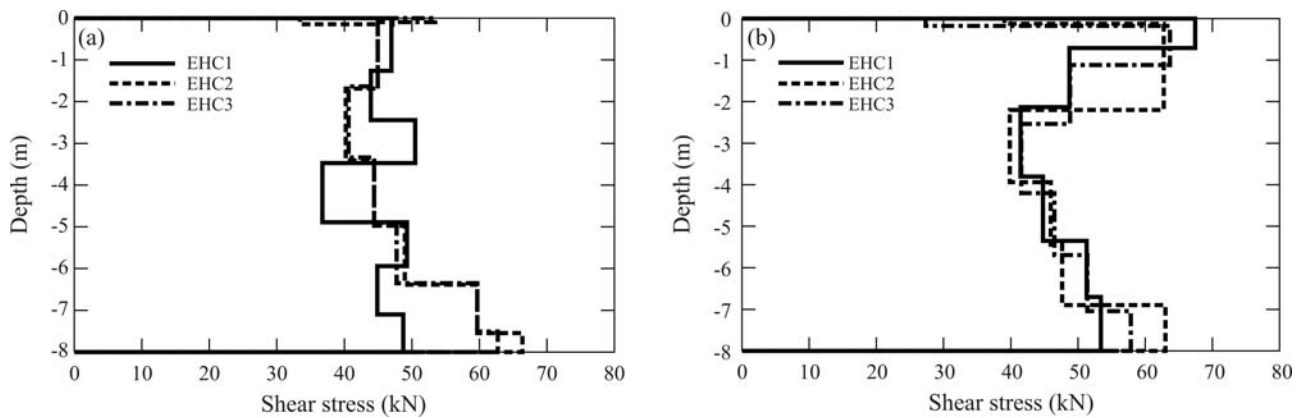


Figure 21 - Lateral friction stress distribution along the shaft - stress state after failure, (a) pile group, (b) piled raft.

The magnitude of increase of the frictional stress has exceeded 20 kN, or more than 50% of the original average (pre failure) values, for some of the simulated cases, which is another good asset of the presence of the surficial raft in piled raft systems. Besides, the level of the lateral friction stresses for the piled rafts, in all compared post failure cases, is higher than the respective level of the pile groups. On the other hand, for situations before failure, both pile groups and piled raft presented mobilized lateral friction resistances of the same range. It is finally noticed, when comparing post and pre failure events for all studied systems, that the mobilized lateral friction resistance is slightly increased when approaching failure.

This subsection enabled an envision of the differential behavior of the systems, at pre and post failure events, when considering (or not) a close contact of the raft with the surficial soil. Even with a surficial weak layer, piled raft systems will behave “better” in cases where the system eventually fails in geotechnical terms. Upon failure, the upper zone of the piles of piled raft systems will have a greater lateral friction mobilization than equivalent values from standard pile groups. On working conditions, on the other hand, both systems will operate similarly, with closer values of mobilized average lateral frictions along pile shaft.

Indeed, the simulations have shown slightly higher frictions for the piles of the pile groups, since, as commented in the previous item, more load is absorbed by such piles in comparison to the piles of the piled raft systems (as the load in such systems is also shared with the raft).

On general terms, and considering the mobilized soil resistance shared by the system components (raft, pile tip and shaft, and soil) and the distribution of mobilized lateral friction at distinct load levels, it is concluded that piled raft systems will behave slightly better than standard pile groups in conditions similar to those tested in Brasília.

5. Conclusions

Three-dimensional finite element analyses of a single pile, of various types of pile groups and of piled rafts founded in typical tropical porous clay of the Federal District of Brazil were presented and discussed in this paper. The computations were performed for soil parameters obtained: a) from laboratory and *in situ* tests, b) via backward analysis performed by a semi analytical method implemented in FINE Geo4 software and c) via backward analysis of a single CFA pile performed in Plaxis 3D Foundation. In this comparison the set of laboratory and *in situ* parameters failed to model the field tests with a sufficient accuracy.

Better results were obtained by using the back analyzed values, especially those from Plaxis 3D.

Hence, a reasonable approach for choosing soil parameters as input to the FEM model should consist of two alternatives: In the first alternative, soil parameters could be estimated from geotechnical tests or obtained by a simple backward calculation by means of an adequate semi-analytical method, such as the one implemented in FINE Geo4. As a better alternative, a backward analysis of a load test in an isolated pile should be made, using the same software that will perform the analysis of the entire foundation system.

The impact of the group effect of closely constructed piles on the overall bearing capacity proved to be negligible from a practical point of view, based on the numerical simulations. Nevertheless, such effect slightly influences the pre-failure stiffness of the pile group. More notable is the effect of the top raft when it is in contact with the underlying soil layer. The raft had the ability to increase the bearing capacity by approximately 15% for the presented configurations of foundation systems. The pre-failure settlement was also decreased by approximately 7% when compared to traditional pile groups. More significant contribution of the raft appears at post failure stages. Piled rafts reduce post-failure displacements more effectively and soften the abrupt fragile type failure observed in the case of traditional piled groups founded in this collapsible clay.

Lateral friction distribution along the piles, load shares between the elements of the system (raft, piles and soil), bearing capacity, and the overall behavior, are indeed improved by having the raft in close contact with the surficial soil, in other words, by designing the foundation system as a piled raft one. This is valid for load levels at working or, in extreme cases, failure conditions, and denotes the necessity that foundation practitioners have to start considering this type of design approach on daily practice. At least for more substantial foundation works, as bridges, large buildings, etc., where the raft will be, indeed, placed on top of a more competent soil stratum.

The results of this paper prove that, although not straight forward, it is possible to simulate and forecast the behavior of piled raft systems founded in rather complex soils, as the Brasília porous clay, and to compare the results directly to simulations of the same systems when behaving as standard pile groups. It also proves that a feasibility of the analysis can be reached by using readily available parameters from pile load tests or site and laboratory investigations, allied to a standard commercial software. Of course, some common sense and previous experience is desired, but this aspect is valid in all facets of the geotechnical design.

It finally emphasizes that there is a large benefit in designing with the (piled raft) approach advocated herein, especially on soils that are better suited to assist the surficial raft in sustaining part of the superstructure loads, as stiff

clays, dense sands, laterized tropical soils or residual crusts. Moreover, more recent studies, as those published by Cunha *et al.* (2007) and Cordeiro *et al.* (2008), also demonstrate the large potential and beneficial aspects that exists in adopting piled raft methodology to simulate, and reinforce, foundation groups with one or more defective piles.

Although more research still needs to be done in this area, this paper also proves that the level of knowledge which exists today is more than enough to allow foundation designers to take sharp decisions in the design of foundations of any complexity, looking forward to economy allied to a better performance of such structures. In other words, as the “Star Trek” series used to mention in their openings, it is now the time “to boldly go where no one has gone before”

Acknowledgments

The financial support provided by the grant n. 1ET410430516 awarded by the Czech Academy of Sciences is gratefully acknowledged. The first author would also like to express his gratitude to all staff of the Geotechnical Post Graduation Program of the University of Brasília, and the Brazilian sponsorship organization CAPES for the support received during the period spent at this workplace. The second author thanks the sponsorship organizations CNPq, CAPES and UnB Foundation Finatec for all related support in this and all other studies carried out by him, and the last author acknowledges the support given by several engineering companies from the Federal District in carrying out all field related tasks, as the companies Embre, Soltec, OAS, WRJ, Sulamericana and Infraso Engineering Ltd. It is also thanked by this same author the scholarship kindly provided by CAPES during his D.Sc. studies at UnB.

References

- Anjos, G.J.M. (2006) Study of the Behavior of Foundations Bored on Tropical Soils. D.Sc. Thesis, Universidade de Brasília, Brasília, 341 pp. (In Portuguese).
- Anjos, G.J.M.; Cunha, R.P.; Kuklík, P. & Miroslav, B. (2006) Numerical evaluation of bored piles in tropical soils by means of the geotechnical engineering “GEO4” Fine software. Proc. 3rd European Conf. on Computational Mechanics Solids, Struct. and Coupled Prob. in Eng., Lisboa, CD Rom, 10 pp.
- Cordeiro, A.F.; Cunha, R.P.; Broucek, M. & Sales, M.M. (2008) Piled rafts with defective piles: influence of reinforcement systems. Foundations: Proceedings of the Second BGA International Conference on Foundations, ICOF2008, Dundee. v. 1, pp. 485-492.
- Cunha, R.P. & Sales, M.M. (1998) Field load tests of piled footings founded on a tropical porous clay. Proc. 3rd International Geotechnical Seminar on Deep Foundation on Bored and Auger Piles, Ghent, v. 1, pp. 433-438.

- Cunha, R.P.; Cordeiro, A.F.; Sales, M.M. & Small, J.C. (2007) Parametric analyses of pile groups with defective piles: Observed numerical behaviour and remediation. Proc. 10th Australia New Zealand Conference on Geomechanics, Brisbane, v. 1, pp. 454-459.
- Cunha, R.P.; Bezerra, J.E. & Zhang, H.H. (2006) Influence of the relative stiffness pile/soil (Kps) in conventional pile groups and of the "pile draft" type. Proc. XIII Brazilian Congress on Soil Mechanics and Geotechnical Engineering, Curitiba, v. 2, pp. 793-798 (In Portuguese).
- Cunha, R.P.; Bezerra, J.E.; Zhang, H.H. & Small, J.C. (2004) Back analyzed parameters from piled foundations founded on tropical porous clay. Int. Conf. on Cooperation and Innovation in the Geo-Industry. ASCE Geot. Special Pub., n. 124, pp. 1003-1014.
- Cunha, R.P.; Jardim, N.A. & Pereira, J.H.F. (1999) *In situ* characterization of a tropical porous clay via dilatometer tests. Geo-Congress 99 on Behavioral Characteristics of Residual Soils. ASCE Geotechnical Special Publication n. 92, pp. 113-122.
- Cunha, R.P.; Poulos, H.G. & Small, J.C. (2001) Investigation of design alternatives for a piled raft case history. ASCE Journal of Geotechnical and Geoenvironmental Engineering, v. 127:8, p. 635-641.
- Cunha, R.P.; Small, J.C. & Poulos, H.G. (2000a) Class C analysis of a piled raft case history in Gothenburg, Sweden. Year 2000 Geotechnics - Geotechnical Engineering Conference, Bangkok, v. 1, pp. 271-280.
- Cunha, R.P.; Small, J.C. & Poulos, H.G. (2000b) Parametric analysis of a piled raft case history in Uppsala, Sweden. IV Seminar of Special Foundations and Geotechnics, São Paulo, v. 2, pp. 381-390.
- Cunha, R.P. & Zhang, H.H. (2006) Behavior of piled raft foundation systems under a combined set of loadings. Proc. 10th Int. Conf. on Piling and Deep Foundations, Amsterdam, v. 1, pp. 242-251.
- Fine (2007) Geo4 Software. Fine Civil Engineering Software Ltd. <http://www.fine.cz/>.
- Mandolini, A. (2003) Design of piled rafts foundation: Practice and development. Proc. 4th International Geotechnical Seminar on Deep Foundation on Bored and Auger Piles, Ghent, pp. 59-80.
- Mandolini, A. & Viggiani, C. (1997) Settlement of piled foundations. Géotechnique, v. 47:4, p. 791-816.
- Mota, N.M.B. (2003) Advanced *in situ* Tests in the Unsaturated and Porous Clay of Brasília: Interpretation and Application Into Foundation Design Projects. D.Sc. Thesis, Universidade Brasília, Brasília, 336 pp. (In Portuguese).
- Ottaviani, M. (1975) Three-dimensional finite element analysis of vertically loaded pile groups. Géotechnique, v. 25:2, p. 159-174.
- Plaxis (2007) Plaxis Finite Element Code for Soil and Rock Analyses. <http://www.plaxis.nl/>.
- Poulos, H.G. (1998) The pile-enhanced raft - An economical foundation system. Proc. XI Brazilian Congress on Soil Mechanics and Geotechnical Engineering, Brasília, v. 4, pp. 27-43.
- Randolph, M.F. (1994) Design methods for pile groups and piled rafts. State of art report. Proc. 13th Intern. Conf. on Soil Mechanics and Foundation Eng., New Delhi, v. 5, pp. 61-82.
- Sales, M.M.; Cunha, R.P. & Jardim, N.A. (1999) Analysis of piled footing tests on a tropical porous clay. Proc. XI Panamerican Conference on Soil Mechanics and Geotechnical Engineering, Foz do Iguaçu, v. 3, pp. 1395-1402.
- Sales, M.M.; Cunha, R.P.; Poulos, H.G. & Small, J.C. (2005) Simplified approach for load-settlement curve estimation of piled rafts. Solos e Rochas, v. 28:1, p. 73-83.